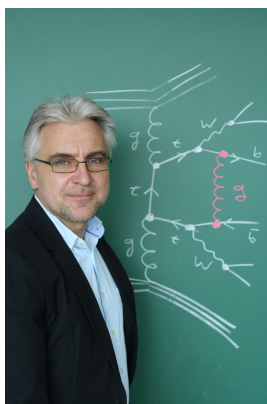


STANDARD MODEL THEORY

STEFAN DITTMAIER

*Albert-Ludwigs-Universität Freiburg, Physikalisches Institut,
79104 Freiburg, Germany*



Recent progress in the field of precision calculations for Standard Model processes at the LHC is reviewed, highlighting examples of weak gauge-boson and Higgs-boson production, as discussed at the 27th Rencontres de Blois, 2015.

1 Introduction

After Run 1 of the LHC, the Standard Model (SM) is in better shape than ever in describing practically all phenomena in high-energy particle physics. The search for new physics, thus, has to proceed with precision at the highest possible level, in order to reveal any possible deviation from SM predictions. To this end, both QCD and electroweak (EW) corrections have to be included in cross-section predictions.

The field of perturbative precision calculations has experienced tremendous progress in recent years in various directions. Next-to-leading-order (NLO) QCD calculations have been automated up to particle multiplicities of roughly 4–6 (depending on the complexity of the process) upon combining multi-purpose Monte Carlo generators or integrators with automated tools for the generation of multi-leg one-loop matrix elements. For NLO EW corrections the automation is in progress as well. At the next-to-next-to-leading-order (NNLO) level more and more complete QCD calculations have been completed for various $2 \rightarrow 2$ particle scattering processes, and for $2 \rightarrow 1$ processes even first results at next-to-next-to-next-to-leading order (NNNLO) are presented. This progress in fixed-order calculations goes in parallel with new achievements in the resummation of leading corrections to all perturbative orders. On the one hand, analytic QCD resummations were continuously pushed to higher and higher levels. On the other hand, fixed-order calculations were matched to QCD parton showers, where the NLO level meanwhile follows standard procedures and the frontier moved on to NNLO¹. In cases where the matching of NLO corrections with parton showers does not yet deliver sufficient precision in the first few jet

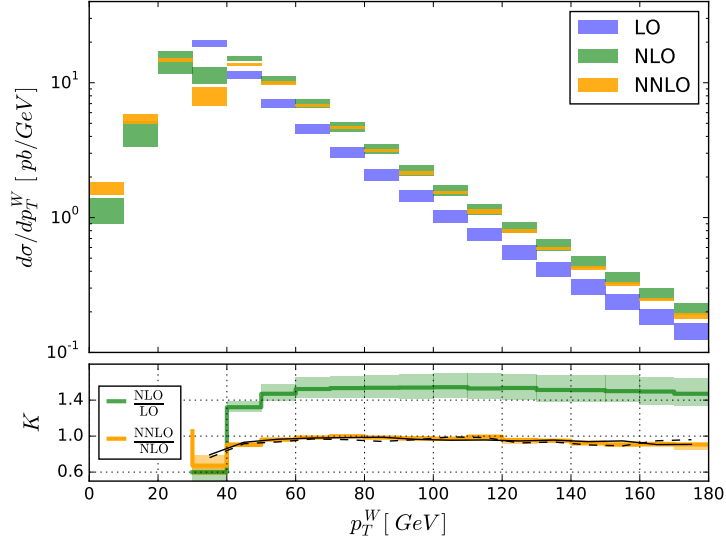


Figure 1 – NNLO QCD prediction for the transverse-momentum (p_T) spectrum of the W boson in $W^+(\rightarrow \ell\nu)+\text{jet}$ production at the LHC at 8 TeV and corresponding K factors (taken from Boughezal et al.²). The factorization and renormalization scales are set to $\mu = M_W$ and simultaneously varied by a factor of 2 up and down in the shown uncertainty bands.

multiplicities, improvements are often obtained upon merging NLO calculations for producing a specific event topology together with $n = 0, 1, 2, \dots$ jets, thereby carefully avoiding double-counting of jet activity.

In this short review, some highlights in the recent progress in fixed-order calculations are summarized. In detail, advances in precision calculations for the production of W/Z bosons + jets and of weak gauge-boson pairs are discussed as well as recent results on the Higgs-boson production rate and the corresponding transverse-momentum spectrum.

2 Weak-gauge-boson production

2.1 W/Z production in association with hard jets

The production of W or Z bosons in association with hard jets represents an important class of standard processes at the LHC, both as testground for jet dynamics in QCD and as background process to many searches. The corresponding SM predictions experienced an enormous boost in precision in recent years.

After an effort over many years, very recently the QCD-based predictions for W/Z+1jet were pushed to the NNLO level^{2,3}. As one of the central results, Fig. 1 shows the transverse-momentum spectrum of the W boson in $W^+(\rightarrow \ell\nu)+\text{jet}$ production at the LHC at 8 TeV at LO, NLO, and NNLO². While fixed-order predictions generally are not able to describe the range of low p_T^W , for intermediate and large p_T^W the perturbative series shows nice convergence. For p_T^W in the range $50 \text{ GeV} \lesssim p_T^W \lesssim 180 \text{ GeV}$, the QCD corrections are $\sim 40\%$ at NLO, but only a few percent at NNLO, reducing the residual scale uncertainty from $\sim 20\%$ at NLO to only few percent at NNLO. The pattern of the NNLO QCD corrections to Z+1jet production is very similar³. To bring the overall theory uncertainty to the level of the missing QCD corrections of some percent, in particular, the EW corrections at the NLO level have to be taken into account. They are known not only for on-shell W/Z bosons⁴, but also including all off-shell and decay effects⁵.

In the completion of the NNLO QCD calculations the major obstacle was the extraction of infrared (IR) singularities from the real double-emission and the real-virtual contributions and their cancellation against their virtual counterparts. The major breakthrough in the calculation

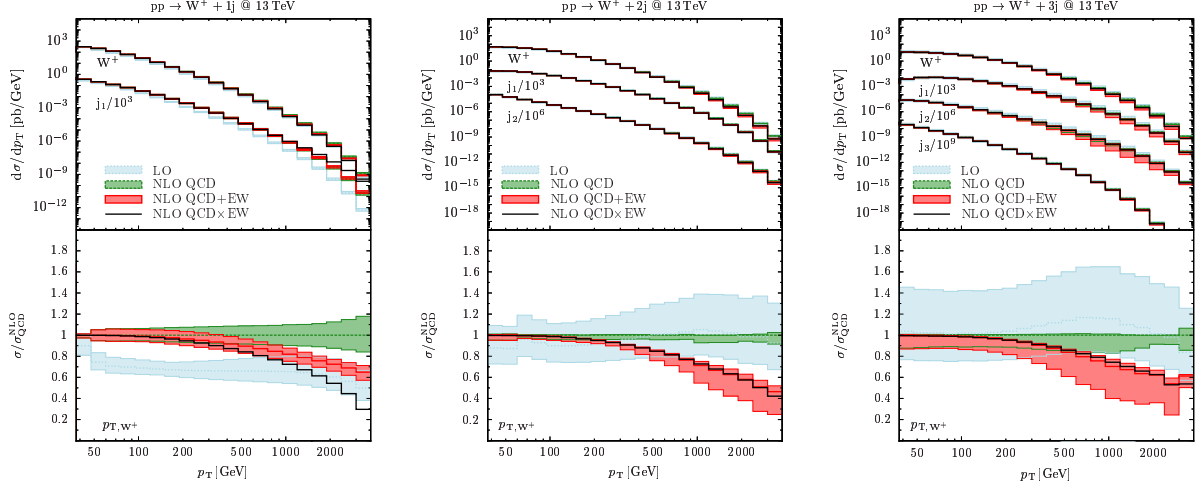


Figure 2 – Transverse-momentum distributions for the production of $W^+ + 1, 2, 3$ jets in LO and including NLO QCD and EW corrections (taken from Kallweit et al. ¹⁴).

for $W+1$ jet production ² was the invention of a new technique called “jettiness subtraction” ⁶, where the soft/collinear IR singularities are isolated by some cut on the “jettiness” ⁷ \mathcal{T}_N of the events,

$$\mathcal{T}_N = \sum_k \min_i \left\{ \frac{2p_i \cdot q_k}{Q_i} \right\}. \quad (1)$$

The procedure works as follows: First the number N of jets is determined with any jet algorithm, thereby defining N light-like reference momenta p_i (+2 beam momenta for pp collisions). Then \mathcal{T}_N is calculated from the sum over all parton momenta q_k , taking appropriate scales Q_i to characterize the hardness of the jets. The limit $\mathcal{T}_N \rightarrow 0$ corresponds to exactly N resolved jets and is independent of the jet algorithm. The phase space can, thus, be partitioned into regions with $\mathcal{T}_N < \mathcal{T}_N^{\text{cut}}$ and $\mathcal{T}_N > \mathcal{T}_N^{\text{cut}}$, where the former isolates the IR-singular regions where factorization properties of the amplitudes can be used to analytically integrate over the singular degrees of freedom. Since the structure of this procedure is rather generic, the technique, which has been suggested in different variants ^{6,8}, should find more applications in forthcoming NNLO calculations. We note in passing that the NNLO calculation for $Z+1$ jet production ³ was based on a different well-established approach for the treatment of IR singularities known as “antenna subtraction” ⁹.

Turning to higher jet multiplicities, the NLO level represents the state of the art. NLO QCD predictions even went up to 3 ¹⁰, 4 ¹¹, and 5 ¹² jets in association with a W or Z boson, at least in leading-colour approximation. Concerning EW corrections, NLO predictions were recently calculated for $Z+2$ jet production ¹³ (with Z-boson decays and off-shell effects) and $W+1,2,3$ jet production ¹⁴ (for on-shell W bosons). Exemplarily Fig. 2 compares the NLO QCD and EW corrections to the W-boson transverse-momentum distribution for the three different jet multiplicities. Normalizing the relative corrections to NLO QCD, the plots reflect the well-known “giant QCD K factor” for $W+1$ jet, but QCD corrections at the 10% level for 2 and 3 jets. The scale uncertainty is roughly $\sim 10\%$ ($\sim 20\%$) for $p_{T,W}$ up to 500 GeV (2 TeV). The EW corrections show the generic feature to grow large and negative for increasing $p_{T,W}$, reaching tens of percent in the TeV range, as consequence of the EW Sudakov logarithms at high scales, which are due to the soft/collinear exchange of virtual W/Z bosons. There are, however, other mechanisms as well that potentially cause sizeable EW corrections at higher energies, such as interferences with diagrams where jets are initiated by EW particles or channels with photons in the initial state. Details about those effects, including also other observables, are discussed by Kallweit et al. ¹⁴. Note also the difference between the two variants of combining QCD and EW corrections based on mere addition (red curves) or assuming factorization (black curves).

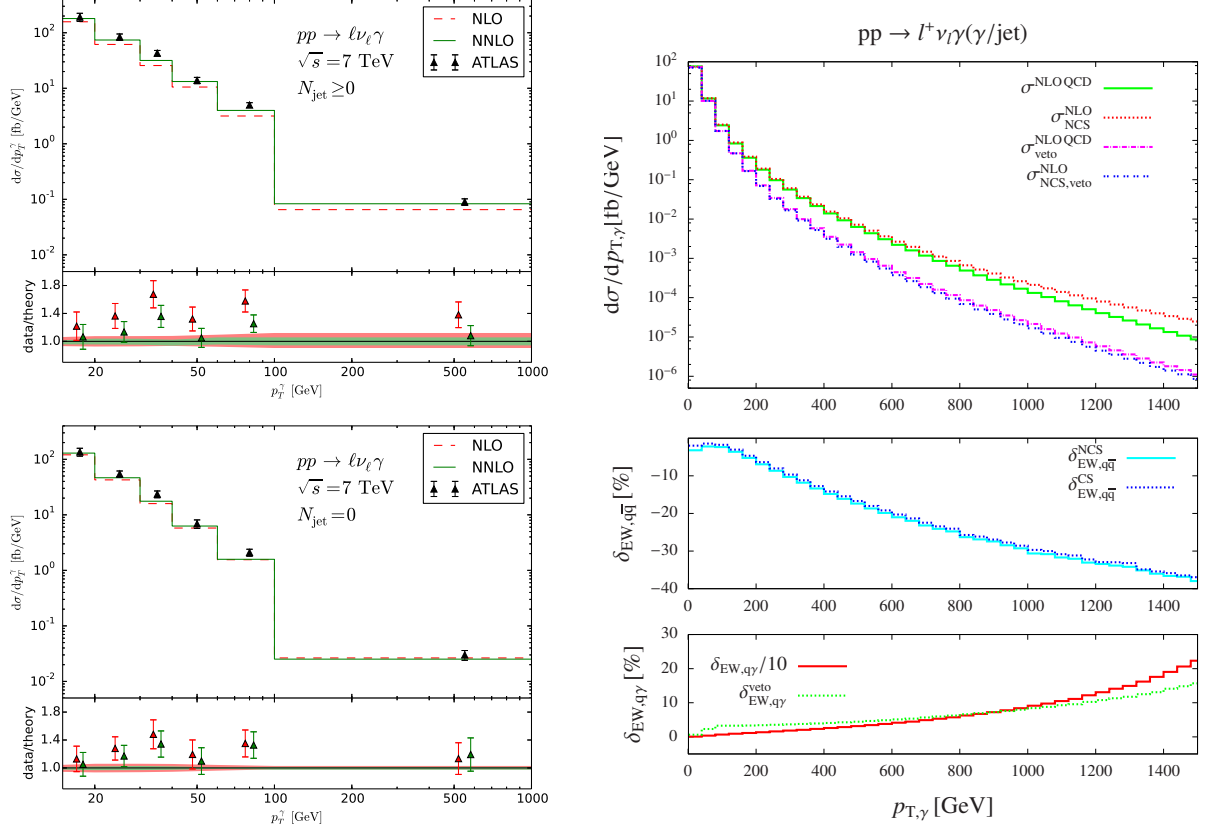


Figure 3 – Transverse-momentum distribution of the photon in $W^+ + \gamma$ production at the LHC at NLO and NNLO confronted with LHC data (left) and including various types of NLO EW corrections (right) (taken from Grazzini et al.¹⁸ and Denner et al.²⁷, respectively).

For $W+1\text{jet}$ production the difference becomes large, since both QCD and EW corrections are large. While there are good arguments favouring factorization, since large universal QCD and EW effects factorize, ultimately the uncertainty can only be resolved by an NNLO QCD–EW calculation.

For single- W/Z production a strategy for calculating NNLO QCD–EW corrections was worked out in Ref.¹⁵ for W/Z bosons near their mass shell. Already this relatively simple example at NNLO reveals¹⁶ that the success of a naive factorization of relative NLO QCD and NLO EW correction factors is rather limited, since the naive factors do not account for the accumulation of jet and photon recoils in the double-real corrections.

2.2 Electroweak gauge-boson pair production

We turn to pair production processes of EW gauge bosons where NNLO QCD predictions experienced a breakthrough in the previous two years with completed calculations for $Z/W\gamma$ ^{17,18}, ZZ ¹⁹, WW ²⁰ based on on-shell W/Z gauge bosons, and recently for ZZ ²¹ even for off-shell Z bosons. The issue of extracting and cancelling IR singularities in these calculations was accomplished by so-called “ q_T subtraction”²², which exploits the fact that QCD emission in processes with colour-neutral final states can be isolated in the limit where jets have small transverse momentum.

The l.h.s. of Fig. 3 shows a confrontation of such a prediction for $W\gamma$ production with ATLAS data collected at an energy of 7 TeV. Already these data, which reach only up to few 100 GeV in the hard-photon transverse momentum, favour the NNLO over the NLO prediction, but upcoming data from LHC Run 2 will deepen the reach in p_T^γ enormously with lower statistical errors, leading to a more stringent test of the predictions. At that level, the NLO EW corrections

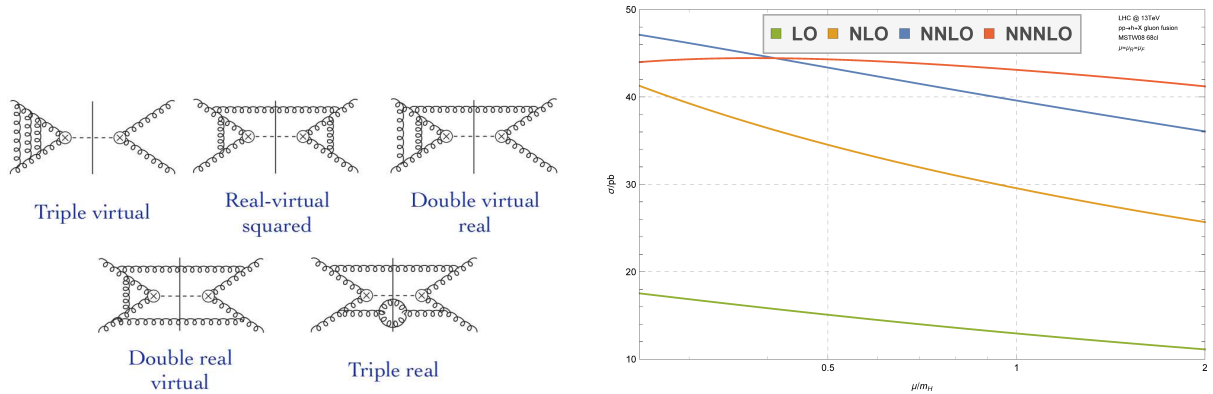


Figure 4 – Relevant diagrammatic structures (left) for NNNLO QCD corrections to Higgs production via gluon fusion, $gg \rightarrow H$, and scale dependence ($\mu = \mu_{\text{ren}} = \mu_{\text{fact}}$) of the corresponding pp cross section at LO, NLO, NNLO, and NNNLO (taken from Anastasiou et al.³⁴).

will become significant as well. They are known for $Z\gamma/WW/WZ/ZZ$ ²³ with stable W/Z bosons, for $Z/W\gamma$ ²⁴ and WW ²⁵ in leading pole approximation^a, and for $W\gamma$ ²⁷ fully including decay and off-shell effects. The r.h.s. of Fig. 3 shows results from the latter calculation of the NLO EW corrections, demonstrating again large negative EW corrections for increasing p_T^γ . The bottom panel additionally reveals a surprisingly large impact of photon-induced collisions from the partonic process $q\gamma \rightarrow W\gamma q$ (with q any quark or antiquark), even in the presence of a jet veto. Since the photon density is rather uncertain ($\sim 100\%$) for large parton momentum fractions²⁸, an improved determination of the photon density is necessary to further stabilize $W\gamma$ predictions in the TeV range.

3 Higgs-boson production

Predictions for the various production channels of Higgs bosons were continuously improved and refined in the last two decades. The basic concepts and results were collected and reviewed in the last years by the LHC Higgs Cross Section Working Group²⁹ and in review articles such as Ref.³⁰. Here we restrict ourselves to a short discussion of the production of a single Higgs boson with or without a hard jet.

3.1 Single-Higgs-boson production

In the SM single-Higgs-boson production at hadron colliders is a loop-induced process where mainly two gluons produce the Higgs boson via a top-quark loop. The mass hierarchy $2m_t \gg M_H$ and the fact that the relevant partonic scattering energy $\sqrt{\hat{s}}$ concentrates in the vicinity of the threshold at M_H implies the possibility to evaluate transition amplitudes in terms of an asymptotic series in inverse powers $1/m_t^n$ of the top quark. This approach can nicely be formalized in the framework of an effective field theory with local Higgs–gluon interactions where the top quark is integrated out. While the m_t -dependence of amplitudes and cross sections are known to NLO for a long time³¹ and to NNLO³² QCD up to the relevant powers in $1/m_t$, the leading contribution (which is of $1/m_t^0$, i.e. a constant in m_t) to the cross section has been recently worked out even to the NNNLO QCD level^{33,34} (see also Ref.³⁵), which documents the first cross-section calculation at this order. The l.h.s. of Fig. 4 shows the relevant types of interference terms contributing to the cross section at this level, whose calculation is of enormous complexity. The integrated partonic cross section is calculated as asymptotic series organized in powers $(1-z)^n$, where $z = M_H^2/\hat{s}$, i.e. virtual and soft-gluon contributions appear at threshold

^aPredictions for the production of massive decaying gauge-boson pairs based on approximated NLO EW corrections are included in HERWIG²⁶.

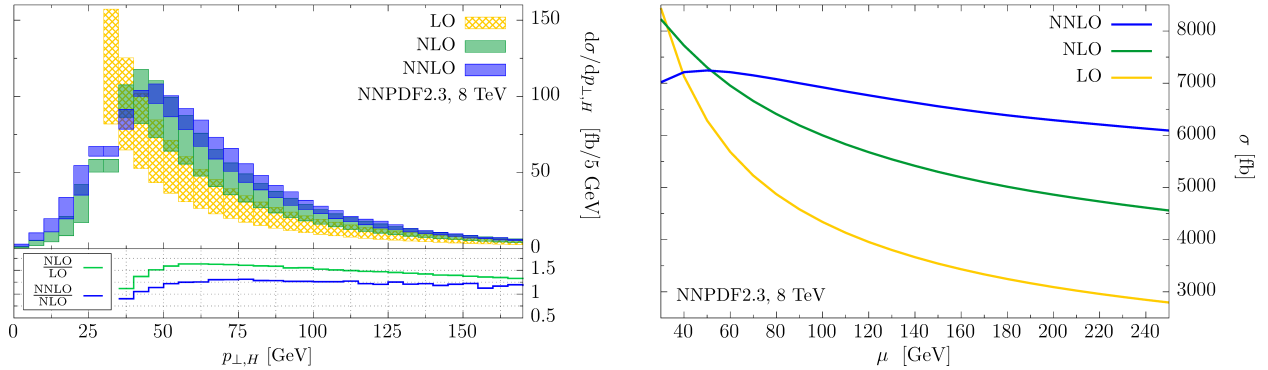


Figure 5 – Prediction for the transverse-momentum spectrum of Higgs-boson production at the LHC at LO, NLO, and NNLO QCD and corresponding K factors (left), and scale dependence (right) of the corresponding integrated cross section (taken from Boughezal et al.³⁹).

where $z \rightarrow 1$. In order to achieve sufficient precision, about 35 terms were required in this series expansion. The scale dependence of the resulting pp cross section goes down from $\sim 9\%$ to $\sim 3\%$ in the step from NNLO QCD to NNNLO QCD, as illustrated on the r.h.s. of Fig. 4, which nicely shows the perturbative convergence from LO through NNNLO. The NNNLO correction itself is $\sim 2\%$ at the scale $\mu = M_H/2$. It is not yet fully understood why the approximate NNNLO result³⁶ based on virtual+soft corrections at $z \rightarrow 1$ in combination with the known high-energy behaviour at $z \rightarrow 0$ does not agree with the full calculation very well.

Another issue in this context concerns the proper estimate of the full theoretical uncertainty which is, e.g., delicate because parton distribution functions extracted from experiment at NNNLO are not available. Moreover, several other effects play a role at this level of precision of few percent, such as the influence of a finite bottom mass (only known to NLO) and the combination with the NLO EW corrections³⁷, which amount to 5% and whose factorization is based on arguments motivated by an effective field theory for $M_H \rightarrow 0$ ³⁸.

3.2 Higgs-boson production in association with a hard jet

The transverse-momentum spectrum of the Higgs boson is an important observable to identify and analyze Higgs-boson events. Since single-Higgs-boson production proceeds via $gg \rightarrow H$ in LO, the Higgs boson can receive a non-vanishing transverse momentum only via the radiation of a jet (or other particles in higher orders). Recently, the QCD predictions of the $p_{T,H}$ spectrum were pushed to the NNLO level^{39,40}, where the IR singularities were treated with so-called sector-improved residue subtraction⁴² in the former calculation (see also Ref.⁴¹) and with jetiness subtraction^{6,8} in the latter.^b Figure 5 summarizes the central results of these calculations. The QCD scale uncertainty of the integrated cross section with $p_{T,\text{jet}} > 30$ GeV (shown on the r.h.s.) goes down from $\sim 23\%$ at NLO to $\sim 9\%$ at NNLO. This behaviour is also observed for the relevant part of the $p_{T,H}$ spectrum, shown in the l.h.s. of Fig. 5, which reveals NNLO QCD corrections of $\sim 20\%$ on top of the NLO prediction. NLO EW corrections to H+jet production, which involve $2 \rightarrow 2$ two-loop amplitudes with many scales, are not yet known, but their size most probably does not exceed the size of the remaining QCD scale uncertainty for not too large transverse momenta.

4 Conclusion

The field of perturbative calculations for particle collisions has developed very rapidly in recent years towards higher and higher precision in many different directions. The process of automating NLO calculations for multi-particle production reached a rather mature state in QCD and

^bNNLO QCD results based on the gg channel only⁴³ were also evaluated with the help of antenna subtraction.

is successfully ongoing on the EW side. Beyond NLO, more and more results at NNLO QCD have become available for $2 \rightarrow 2$ scattering processes, and $2 \rightarrow 1$ processes, such as inclusive Higgs-boson production, are even treated in NNNLO QCD. Selected highlights at this frontier have been briefly discussed in this short article.

Apart from the discussed directions, there was also significant progress in the field of analytic resummations and parton-shower approaches and their combination with fixed-order calculations, an issue that could not be touched here. The same applies to new concepts and techniques of more formal field theory or mathematics as well as all kind of applications to physics beyond the SM, etc. A short article can hardly do justice to the great success of the whole field.

Acknowledgments

I would like to thank the organizers for perfectly setting up the conference at such an inspiring and interesting place like Château Royal de Blois.

References

1. S. Höche *et al.*, Phys. Rev. D **91** (2015) 7, 074015 [arXiv:1405.3607 [hep-ph]]; A. Karlberg *et al.*, JHEP **1409** (2014) 134 [arXiv:1407.2940 [hep-ph]].
2. R. Boughezal *et al.*, Phys. Rev. Lett. **115** (2015) 6, 062002 [arXiv:1504.02131 [hep-ph]].
3. A. Gehrmann-De Ridder *et al.*, arXiv:1507.02850 [hep-ph].
4. J. H. Kühn *et al.*, Nucl. Phys. B **727** (2005) 368 [hep-ph/0507178]; Nucl. Phys. B **797** (2008) 27 [arXiv:0708.0476 [hep-ph]]; W. Hollik *et al.*, Nucl. Phys. B **790** (2008) 138 [arXiv:0707.2553 [hep-ph]]; arXiv:1504.07574 [hep-ph].
5. A. Denner *et al.*, JHEP **0908** (2009) 075 [arXiv:0906.1656 [hep-ph]]; JHEP **1106** (2011) 069 [arXiv:1103.0914 [hep-ph]]; Eur. Phys. J. C **73** (2013) 2, 2297 [arXiv:1211.5078 [hep-ph]].
6. R. Boughezal *et al.*, Phys. Rev. D **91** (2015) 9, 094035 [arXiv:1504.02540 [hep-ph]].
7. I. W. Stewart *et al.*, Phys. Rev. Lett. **105** (2010) 092002 [arXiv:1004.2489 [hep-ph]].
8. J. Gaunt *et al.*, arXiv:1505.04794 [hep-ph].
9. A. Gehrmann-De Ridder *et al.*, JHEP **0509** (2005) 056 [hep-ph/0505111].
10. R. K. Ellis *et al.*, JHEP **0904** (2009) 077 [arXiv:0901.4101 [hep-ph]]; Phys. Rev. D **80** (2009) 094002 [arXiv:0906.1445 [hep-ph]]; C. F. Berger *et al.*, Phys. Rev. Lett. **102** (2009) 222001 [arXiv:0902.2760 [hep-ph]]; Phys. Rev. D **80** (2009) 074036 [arXiv:0907.1984 [hep-ph]]; Phys. Rev. D **82** (2010) 074002 [arXiv:1004.1659 [hep-ph]].
11. C. F. Berger *et al.*, Phys. Rev. Lett. **106** (2011) 092001 [arXiv:1009.2338 [hep-ph]]; H. Ita *et al.*, Phys. Rev. D **85** (2012) 031501 [arXiv:1108.2229 [hep-ph]].
12. Z. Bern *et al.*, Phys. Rev. D **88** (2013) 1, 014025 [arXiv:1304.1253 [hep-ph]]; D. Götz *et al.*, PoS LL **2014** (2014) 009 [arXiv:1407.0203 [hep-ph]].
13. A. Denner *et al.*, JHEP **1501** (2015) 094 [arXiv:1411.0916 [hep-ph]].
14. S. Kallweit *et al.*, JHEP **1504** (2015) 012 [arXiv:1412.5157 [hep-ph]].
15. S. Dittmaier *et al.*, Nucl. Phys. B **885** (2014) 318 [arXiv:1403.3216 [hep-ph]].
16. S. Dittmaier *et al.*, PoS LL **2014** (2014) 045 [arXiv:1405.6897 [hep-ph]].
17. M. Grazzini *et al.*, Phys. Lett. B **731** (2014) 204 [arXiv:1309.7000 [hep-ph]].
18. M. Grazzini *et al.*, JHEP **1507** (2015) 085 [arXiv:1504.01330 [hep-ph]].
19. F. Cascioli *et al.*, Phys. Lett. B **735** (2014) 311 [arXiv:1405.2219 [hep-ph]].
20. T. Gehrmann *et al.*, Phys. Rev. Lett. **113** (2014) 21, 212001 [arXiv:1408.5243 [hep-ph]].
21. M. Grazzini *et al.*, arXiv:1507.06257 [hep-ph].

22. S. Catani and M. Grazzini, Phys. Rev. Lett. **98** (2007) 222002 [hep-ph/0703012].
23. W. Hollik and C. Meier, Phys. Lett. B **590** (2004) 69 [hep-ph/0402281];
A. Bierweiler *et al.*, JHEP **1211** (2012) 093 [arXiv:1208.3147 [hep-ph]]; JHEP **1312** (2013) 071 [arXiv:1305.5402 [hep-ph]];
J. Baglio *et al.*, Phys. Rev. D **88** (2013) 113005 [arXiv:1307.4331].
24. E. Accomando *et al.*, Eur. Phys. J. C **47** (2006) 125 [hep-ph/0509234].
25. M. Billoni *et al.*, JHEP **1312** (2013) 043 [arXiv:1310.1564 [hep-ph]].
26. S. Gieseke *et al.*, Eur. Phys. J. C **74** (2014) 8, 2988 [arXiv:1401.3964 [hep-ph]].
27. A. Denner *et al.*, JHEP **1504** (2015) 018 [arXiv:1412.7421 [hep-ph]].
28. R. D. Ball *et al.* [NNPDF Collaboration], Nucl. Phys. B **877** (2013) 290 [arXiv:1308.0598 [hep-ph]].
29. LHC Higgs Cross Section Working Group, arXiv:1101.0593 [hep-ph]; arXiv:1201.3084 [hep-ph]; arXiv:1307.1347 [hep-ph].
30. S. Dittmaier and M. Schumacher, Prog. Part. Nucl. Phys. **70** (2013) 1 [arXiv:1211.4828 [hep-ph]].
31. D. Graudenz *et al.*, Phys. Rev. Lett. **70** (1993) 1372. M. Spira *et al.*, Nucl. Phys. B **453** (1995) 17 [hep-ph/9504378].
32. R. V. Harlander and K. J. Özzeren, JHEP **0911** (2009) 088 [arXiv:0909.3420 [hep-ph]];
A. Pak *et al.*, JHEP **1002** (2010) 025 [arXiv:0911.4662 [hep-ph]].
33. C. Anastasiou *et al.*, JHEP **1503** (2015) 091 [arXiv:1411.3584 [hep-ph]].
34. C. Anastasiou *et al.*, Phys. Rev. Lett. **114** (2015) 212001 [arXiv:1503.06056 [hep-ph]].
35. B. Mistlberger, these proceedings.
36. M. Bonvini *et al.*, J. Phys. G **41** (2014) 095002 [arXiv:1404.3204 [hep-ph]].
37. S. Actis *et al.*, Phys. Lett. B **670** (2008) 12 [arXiv:0809.1301 [hep-ph]].
38. C. Anastasiou *et al.*, JHEP **0904** (2009) 003 [arXiv:0811.3458 [hep-ph]].
39. R. Boughezal *et al.*, Phys. Rev. Lett. **115** (2015) 8, 082003 [arXiv:1504.07922 [hep-ph]].
40. R. Boughezal *et al.*, Phys. Lett. B **748** (2015) 5 [arXiv:1505.03893 [hep-ph]].
41. F. Caola, these proceedings.
42. M. Czakon, Phys. Lett. B **693** (2010) 259 [arXiv:1005.0274 [hep-ph]];
R. Boughezal *et al.*, Phys. Rev. D **85** (2012) 034025 [arXiv:1111.7041 [hep-ph]];
M. Czakon and D. Heymes, Nucl. Phys. B **890** (2014) 152 [arXiv:1408.2500 [hep-ph]].
43. X. Chen *et al.*, Phys. Lett. B **740** (2015) 147 [arXiv:1408.5325 [hep-ph]].